Operator Splitting of Advection and Diffusion on Non-Uniformly Coarsened Grids

Vera Louise Hauge Jørg Espen Aarnes Knut–Andreas Lie

June 30, 2008

Abstract

High-resolution geological models of subsurface reservoirs typically contain much more details than can be used in conventional reservoir simulators. Geomodels are therefore upscaled before flow simulation is performed. Here, we present a non-uniform coarsening strategy to upscale geomodels, where the coarse grid is generated by grouping cells in the fine-scaled geomodel selectively into connected coarse blocks, with some minimum volume and with the total flow through each coarse block bounded above. Transport is then modeled on this simulation grid. For purely advective flow, the coarsening strategy has been shown to be robust, allowing for both accurate and fast transport simulations of highly heterogeneous and fractured reservoirs.

Here, we consider advection-dominated two-phase flow, where the capillary diffusion is discretized separately from the advective and gravity terms using operator splitting. In particular, we investigate different damping strategies of the diffusive term to counteract overestimation of the diffusion operator on the coarse grid, this to ensure accurate diffusion modelling in the transport solver.

Introduction

High-resolution geomodels of subsurface reservoirs typically contain much more details than what can be used by conventional simulators. Geomodels are therefore upscaled to simulation models of considerably reduced size to enable flow simulation. In this paper we focus on coarsening of grids to be used for computing fluid transport. Aarnes et al. (2007a) recently presented a flow-based coarsening method that preserves the large-scale flow patterns in the geomodel and maintains a high information content. The method assumes that the flow field is known on the geological grid. Thus, the pressure equation has been computed either using a standard pressure solver on the fine grid or with a multiscale method (Aarnes et al., 2007b) that provides a fine-grid velocity field from a coarse-grid solution.

Given a fine-grid flow field, coarse blocks are generated automatically by grouping together cells in the fine-scaled geomodel having approximately the same magnitude of flow. The degree of coarsening is determined implicitly by two prescribed numbers: a minimum block volume and a maximum amount of flow allowed through each block. For purely advective flow, the coarsening strategy has shown to be robust, allowing for both accurate and fast transport simulations of highly heterogeneous reservoirs (Aarnes et al., 2007a), also including fractured reservoirs (Hauge and Aarnes, 2007).

Herein, we extend the method to advection-dominated two-phase flow with capillary and gravity effects included. Operator splitting is used to discretize the capillary diffusion separately from the advective and gravity terms. Using a straightforward projection in the coarse-grid discretization of the diffusion operator generally leads to overestimation of the capillary diffusion. We therefore investigate alternatives for correcting the diffusion operator to accurately capture the balance between advective and diffusive forces.

We start by stating the mathematical model and move on to briefly describe the non-uniform grid coarsening strategy. We then discretize the system and explain the different alternatives for damping excessive diffusion. Finally, the accuracy of the different methods is assessed through a few illustrative numerical examples, before we end the paper by a few concluding remarks.

Mathematical model

We consider immiscible and incompressible two-phase flow of water and oil with gravity and capillary effects included. To describe the system, we will use the so-called fractional flow formulation consisting of a pressure equation and transport equation. The pressure equation reads,

$$v + \tilde{\lambda}\nabla p = -(\lambda_o\rho_o + \lambda_w\rho_w)g\nabla z, \quad \nabla \cdot v = q \tag{1}$$

where $v = v_w + v_o$ is the total Darcy velocity, $\tilde{\lambda}\nabla p = \lambda_w\nabla p_w + \lambda_o\nabla p_o$ gives the total pressure, and $q = q_w + q_o$ is the total volumetric source term. The mobilities λ_i are defined as $\lambda_i = Kk_{ri}/\mu_i$, where K is the absolute permeability, k_{ri} the relative permeability (here assumed to be a quadratic curve of the phase saturation S_i), and μ_i denotes the viscosity. The densities ρ_i are assumed constant, g denotes the gravity constant, and z is the vertical coordinate. The pressure equation is accompanied by a transport equation for one of the saturations. It is common to choose the water saturation S_w and drop the subscript. Hence,

$$\phi\frac{\partial S}{\partial t} + \nabla \cdot [f_w\left(v + \lambda_o\nabla p_{cow} + \lambda_o(\rho_o - \rho_w)g\nabla z\right)] = q_w, \tag{2}$$

where ϕ is the porosity, $f_w = \lambda_w/\lambda$ is the fractional flow function, and $p_{cow} = p_o - p_w$ is the capillary pressure, which we here model by

$$p_{cow} = \epsilon 0.9\phi^{-0.9}K^{-0.5}\frac{1-S}{\sqrt{S}}. \tag{3}$$

The system is closed by specifying appropriate boundary conditions and assuming that the two phases fill the void space completely, that is, $S_w + S_o = 1$. Unless stated otherwise, we assume that the computational domain is initially completely oil-saturated, i.e., $S(x, t = 0) = 0$.

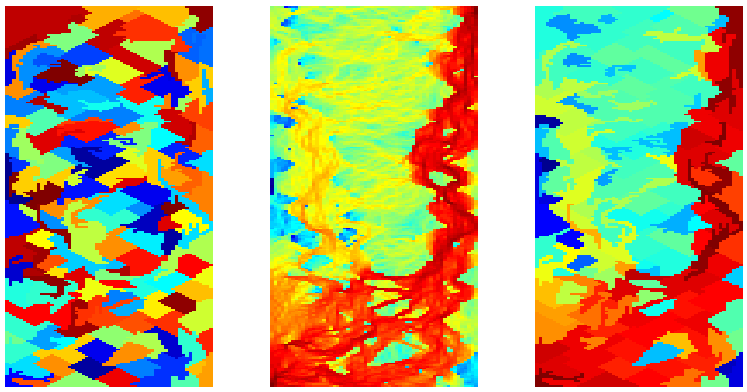

Coarse grid | $\ln |v|$ on fine grid | $\ln |v|$ on coarse grid

Figure 1: An example of a non-uniform coarse grid of 166 blocks along with the logarithm of the velocity on the fine and coarse grid, respectively. (Here, $V_{\min} = 20$ and $G_{\max} = 100$.)

Non-uniform grid coarsening

We consider transport on coarsened simulation grids that are obtained by applying the non-uniform grid coarsening algorithm from (Aarnes et al., 2007a). To distinguish between the coarse and fine grid, we use the term *block* for the coarse grid and *cell* for the fine grid. The algorithm groups cells in the geomodel with equal flow magnitude into coarse blocks. The sizes of the coarse blocks are determined by a lower bound $V_{\min}$ on the volume of each blocks and an upper bound $G_{\max}$ on the total amount of flow through each block. The resulting grid is denoted as non-uniform since the shapes and sizes of the blocks are irregular and vary with the underlying flow field.

An example of a non-uniform coarse grid is given in the left plot of Figure 1. The grid is generated using Layer 46 of Model 2 from SPE 10 (Christie and Blunt, 2001). The total number of coarse blocks is 166. The random coloring does not reflect the underlying permeability field, but is used only to show the shapes and sizes of the grid blocks. In particular, we see irregularly shaped grid blocks, some of which are quite thin and reflect the high-flow channels in the model. The plots of the logarithm of the velocity on both the fine and coarse grid reflect the accuracy that the non-uniform coarse grid reproduces. Note especially that the thin channels in the lower part of the plots are resolved in the coarse grid.

High-resolution geomodels tend to have a large number of layers in the stratigraphic column and can therefore have cells with large aspect ratios. This is a property of the fine grid that may be inherited by the coarse grid. In many cases, flow will follow thin structures in the grid, for instance if the reservoir is fluvial, strongly layered, or contains explicit modeling of fractures. Then, our flow-based method will generate blocks that even accent the large aspect ratios seen in the fine-scale model.

Numerical discretization

Herein, we only consider flow where the viscous term is dominant. In particular, we assume that the capillary pressure effects are adequately modeled through operator splitting. The diffusion term of the saturation equation (2) is therefore treated separately from the viscous and gravity terms. That is, we split the equation into the following system:

$$\phi \frac{\partial S}{\partial t} + \nabla \cdot (f_w v + f_w \lambda_o g(\rho_o - \rho_w)\nabla z) = q_w, \tag{4}$$

$$\phi \frac{\partial S}{\partial t} + \nabla (f_w \lambda_o \frac{\partial p_{cow}}{dS} \nabla S) = 0. \tag{5}$$

In the previous section we saw how the fine-grid flow field was used to compute non-uniform coarsening. Here, we will use the fine-grid fluxes to discretize (4) on the non-uniformly coars-

ened grid. In coarse block B_m, our scheme reads,

$$S_m^{n+1} = S_m^n + \frac{\Delta t}{\int_{B_m} \phi dx} \left[\int_{B_m} q_w(S^{n+1}) dx - \sum_{\gamma_{ij} \subset \partial B_m} \left(V_{ij}(S^{n+1}) + G_{ij}(S^{n+1}) \right) \right],$$

where we have defined the short-hand notation

$$V_{ij}(S) = \frac{\lambda_w(S^w)}{\lambda_w(S^w) + \lambda_o(S^o)} v_{ij}$$

and

$$G_{ij}(S) = g(\rho_o - \rho_w)|\gamma_{ij}| \frac{\lambda_w(S^w)\lambda_o(S^o)}{\lambda_w(S^w) + \lambda_o(S^o)} \nabla z \cdot n_{ij}.$$

Here n_{ij} is the unit normal on the interface γ_{ij} pointing from fine-scale cell T_i to cell T_j, and we have introduced the phase-upwinded saturations S^w and S^o given by

$$S^\alpha = \begin{cases} S|_{T_i} & \text{if } v_{\alpha,ij} \geq 0, \\ S|_{T_j} & \text{if } v_{\alpha,ij} < 0, \end{cases}$$

where $v_{\alpha,ij}$ denotes the phase velocity on the interface γ_{ij} for the water and oil phases, respectively. In other words, the mobility functions λ_w and λ_o are upstream weighted with respect to the fine grid phase velocities, which in turn includes both the viscous flow and the flow driven by gravity.

The nonlinear diffusion equation (5) for the capillary forces takes the following form

$$\phi \frac{\partial S}{\partial t} = \nabla \cdot d(S) \nabla S, \tag{6}$$

where $d(S) = -f_w \lambda_o \frac{\partial p_{cow}}{dS}$ is a non-negative function. For the time discretization, we use a semi-implicit backward Euler method

$$\phi S^{n+1} = \phi S^{n+1/2} - \Delta t \nabla \cdot d(S^{n+1/2}) \nabla S^{n+1}.$$

For spatial discretization of the capillary diffusion we write

$$(\Phi + \Delta t \mathbf{D}) S^{n+1} = \Phi S^{n+1/2}. \tag{7}$$

Here $\Phi = \mathrm{diag}(\phi)$ and $\mathbf{D}$ is a symmetric and semi-positive definite matrix that stems from a cell-centered finite-difference discretization of the semi-elliptic operator $L = -\nabla \cdot d\nabla$. To discretize this operator L on the fine grid, we use a two-point flux approximation scheme. Thus, considering Cartesian grids, we have

$$d_{ij}(S) = -\int_{\gamma_{ij}} d(S) \nabla S \cdot n_{ij} ds \approx |\gamma_{ij}| \tilde{d}(S_i, S_j) \frac{S_i - S_j}{|x_i - x_j|}, \tag{8}$$

where x_i and x_j are the cell centers in cells T_i and T_j, respectively, and $\tilde{d}(S_i, S_j)$ is a suitable average of $d(S_i)$ and $d(S_j)$.

The purpose is to model the capillary diffusion on coarse grids, in particular grids with complex geometries where it is not possible to apply a standard method for discretizing L. We therefore use a projection of the fine-grid discretization onto the coarse grid: Let $\mathbf{R} = r_{ij}$, where r_{ij} equals one if cell T_i is contained in coarse block B_j and zero otherwise. If S_c represents saturation on the coarse grid, then $S_f = \mathbf{R} S_c$ is the corresponding interpolated saturation on the fine grid. If S^{n+1} is the solution of (7) with $S^{n+1/2} = \mathbf{R} S_c^{n+1/2}$, then the projection of S^{n+1} onto the space of piecewise constant functions on the coarse grid is the solution S_c^{n+1} of the following system:

$$[\Phi_c + \Delta t \mathbf{D}_c] S_c^{n+1} = \Phi_c S_c^{n+1/2}, \tag{9}$$

where $\mathbf{D}_c = \mathbf{R}^T \mathbf{D} \mathbf{R}$ and $\Phi_c = \mathbf{R}^T \Phi \mathbf{R}$.

Damping of the diffusion term

Modeling capillary diffusion on the coarse grids using the projection described above with $\mathbf{D}$ defined by (8) will in general overestimate the diffusion. This is because the saturation gradient in (8) is computed on the fine grid, whereas the saturation values represent net saturations in the coarse blocks. For instance, consider a Cartesian fine grid with mesh parameters Δx and Δy and a uniform coarse grid with mesh parameters Δx_c and Δy_c, where each block consists of $n_x \times n_y$ cells. If Γ_{ij} denotes a coarse interface in the x-direction, then the coarse-grid diffusion operator reads

$$d_{c,ij} = -\sum_{n_y} \Delta y d(\gamma_{ij}) \frac{S_i - S_j}{\Delta x} = -\Delta y_c d(\Gamma_{ij}) \frac{S_i - S_j}{\Delta x},$$

while the desired elements would be

$$d_{c,ij} = -\Delta y_c d(\Gamma_{ij}) \frac{S_i - S_j}{\Delta x_c}.$$

It is therefore necessary to damp the diffusion term by a factor of $\frac{\Delta x}{\Delta x_c} = 1/n_x$. Similarly, the corresponding factor will be $\frac{\Delta y}{\Delta y_c} = 1/n_y$ for interfaces in the y-direction.

Motivated by the observation that the capillary diffusion scales with the ratio in the size of the coarse blocks relative to the size of the fine cells, Hauge and Aarnes (2007) proposed the damping factor $(N_b/N_c)^{1/d}$, where N_b denotes the number of blocks, N_c denotes the number of cells, and d is the number of spatial dimensions. Henceforth, we will refer to this as a *crude* damping of the diffusion,

$$\left[\Phi_c + \Delta t \left(\frac{N_b}{N_c}\right)^{1/d} \mathbf{D}_c\right] S_c^{n+1} = \Phi_c S_c^{n+1/2}. \tag{10}$$

In the crude damping we use the factor $(N_b/N_c)^{1/d}$ that is essentially equal to $(n_x n_y)^{-1/2}$ in two dimensions. For uniform Cartesian coarse grids where $n_x \sim n_y$, we see that the crude damping of the diffusion operator indeed results in the desired geometry factor. However, when considering non-uniform coarse grids with complex geometries, this damping factor is not in general sufficient to properly correct the geometric term in (8), consisting of the length $|\gamma_{ij}|$ of the interface between two cells and the distance $|x_i - x_j|$ between the cell centers. Applying the projection of the diffusion operator onto the coarse grid results in a sum of $|\gamma_{ij}|/|x_i - x_j|$ for all fine grid cells in the coarse grid block. Multiplying this sum by $(N_b/N_c)^{1/d}$ does not necessarily reflect the desired geometry terms for a coarse operator, which would be the length of the coarse interface divided by the length of the distance between the block centers.

We therefore suggest a more accurate damping of the capillary diffusion which uses directly the geometry information from the fine grid to correct the coarse-grid diffusion operator. This *fine* damping factor ends up being a matrix with elements for each coarse interface with the precise geometry term for the coarse operator, such that we achieve

$$d_{c,ij} = -|\Gamma_{ij}| d(\Gamma_{ij}) \frac{S_i - S_j}{|C_{B_i} - C_{B_j}|},$$

where C_{B_i} and C_{B_j} are the centers of block i and j, respectively. Figure 2 shows an excerpt of the lower-right corner of the non-uniform coarse grid in Figure 1. The distances between the block centers are marked and indicate the varying geometry terms for each coarse interface.

Numerical simulations

In the following, we investigate numerically the crude damping and the fine damping. For comparison, we include simulations with no damping as well. We first consider a synthetic case that illustrates the effects of the capillary diffusion operator and the damping strategies. Next, we consider saturation solutions in more realistic reservoir models. Finally, the effect of the aspect ratio of reservoirs will be discussed.

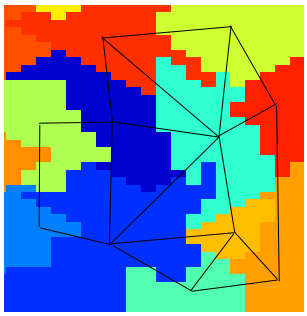

Figure 2: An excerpt of the non-uniform coarse grid in Figure 1 with marked distances between block centers.

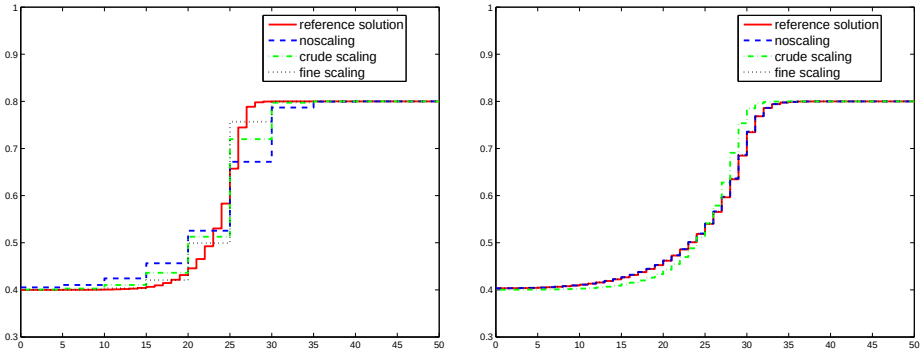

Case 1: overestimation by crude damping

Case 2: underestimation by crude damping

Figure 3: Effect of the damping factors on pure capillary diffusion.

Example 1: *To illustrate the differences between the damping strategies, we consider a synthetic case where the transport is only driven by capillary diffusion. Two uniform coarse grids are considered: In Case 1, the fine grid has* 50×1 *cells with* $\Delta x = \Delta y = 1$*, and the uniform coarse grid has 10 blocks of size* 5×1 *cells. Case 2 has an underlying* 50×5 *fine grid with* $\Delta x = \Delta y = 1$*, and this time the uniform coarse grid consists of 50 blocks, each with* 1×5 *cells. Both cases thus have blocks with more cells in one direction than in the other, such that we do not have* $n_x \sim n_y$*. The crude damping factor* $(N_b/N_c)^{1/d}$ *is in both cases equal to* $1/\sqrt{5}$*.*

We consider reservoirs where half of the reservoir has initial saturation equal to 0.4 for $x < 25$ *and saturation 0.8 for* $x \geq 25$*. Figure 3 shows the saturation profile along the* x*-direction for both cases after some diffusion steps. In Case 1, where* $\Delta x/\Delta x_c = 0.2$*, we observe that using no damping results in considerable overestimation of capillary diffusion. Using the crude damping factor of* $1/\sqrt{5}$ *does not counteract for this overestimation sufficiently. On the other hand, fine damping corrects for the overestimation to a larger degree. For Case 2, we have that* $\Delta x/\Delta x_c = 1$*. The crude damping therefore* underestimates *the capillary diffusion, while the fine damping in fact coincides with no damping and reproduces the correct saturation profile.*

Example 1 illustrates how the relationship between n_x and n_y, when $n_x \not\sim n_y$, affects the crude damping factor, and motivates for using the fine damping strategy. We stress that the flow in this example is purely driven by capillary diffusion and thus shows an exaggerated effect. When advection dominates the fluid flow, then the effect of capillary diffusion is smaller. In the next example, we consider more realistic reservoir models to evaluate the effect of the damping strategies used with the non-uniform coarsening.

Table 1: L^2 error of saturation in different reservoirs.

Model	Fractures	Upscaling	No damping	Crude damping	Fine damping
Homogeneous	no	23	0.0332	0.0295	0.0294
Homogeneous	yes	21	0.0387	0.0277	0.0270
SPE model	no	35	0.0608	0.0385	0.0316
SPE model	yes	30	0.0216	0.0162	0.0123

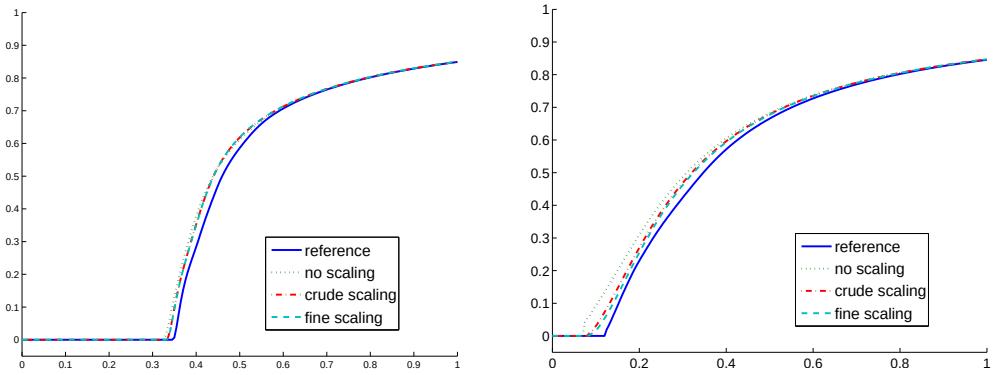

Figure 4: Water cut curves for the homogeneous model with fractures (left) and the SPE model without fractures (right).

Example 2: *We consider quarter five-spot reservoirs with both homogeneous and heterogeneous permeability fields, without and with high-flow fractures. Horizontal and vertical fractures are generated stochastically and are represented as connected paths of cells. For the homogeneous model, we have a uniform permeability field of 1 mD on a uniform* 100×100 *grid, with fractures having a permeability of 1000 mD. For the heterogeneous model, we use Layer 46 from Model 2 of SPE 10 (Christie and Blunt, 2001), referred to as the SPE model. Here, the fractures are assigned the maximum permeability of the channels. In all four cases, we model a relatively strong capillary diffusion with* $\epsilon = 10^{-4}$ *in the definition of capillary pressure (3). We simulate the transport with both advection and diffusion on non-uniform coarse grids using 20 pressure steps and 10 saturation substeps. Time is measured in PVI (pore volume injected).*

Table 1 reports L^2 *errors of the saturations relative to a fine-scale reference solution measured at the end of the simulations. The error measures show that crude damping is slightly more accurate than no damping. Furthermore, fine damping is also only slightly more accurate than the crude damping. However, the overall improvement of the fine damping has to be evaluated together with the additional computation which is required, compared to just using a single factor.*

Figure 4 shows the water cut curves of the homogeneous model with fractures and Layer 46 of the SPE model without fractures. Here we observe the same tendency as in Table 1 with only slightly more accurate performance of the fine damping than crude damping.

In reservoir models as considered in Example 2, which have fine-grid cells with unit aspect ratios, the effect of the crude damping is almost as good as the fine damping and could to a large extent be considered as sufficient. Unfortunately, this is not the case for grids with larger aspect ratios, as are typically seen in (high-resolution) geomodels. High aspect ratios in the fine grid will be preserved in the coarse grid, but since the coarse blocks typically are non-uniform and deviate from a rectangle (or hexahedron in 3D), the errors resulting from using wrong geometrical information (as discussed above) will aggravate with increasing aspect ratios.

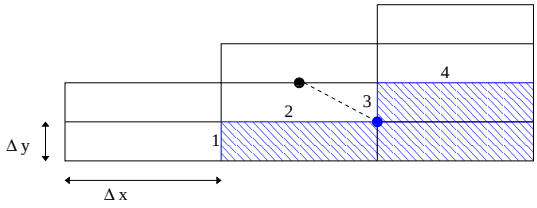

Figure 5: Two coarse grid blocks, with marked distance between the block centers.

To illustrate the effect of large aspect ratios, we first consider a coarse interface in a non-uniform grid with $\Delta x \gg \Delta y$. An illustrating interface is shown in Figure 5 between two coarse blocks. The block centers are marked with dots. Letting the blue-shaded block be denoted i and the white block be denoted j, we want to compute the saturation gradient across the coarse interface consisting of the fine interfaces numbered as 1, 2, 3 and 4 in the figure. The coarse diffusion element in $\mathbf{D}_c$ sums up to be (disregarding the diffusion flux function and the length of the interface, which will be correctly computed)

$$(S_i - S_j)\left(\frac{2}{\Delta x} + \frac{2}{\Delta y}\right) = (S_i - S_j)\left(2\Delta y(\frac{1}{a} + 1)\right),$$

where $a = \frac{\Delta x}{\Delta y}$. The actual distance between the block centers is

$$\sqrt{\Delta y^2 + \left(\frac{\Delta x}{2}\right)^2} = \Delta y\sqrt{1 + \frac{1}{4}a^2} \approx \Delta y\frac{1}{2}a,$$

assuming $a \gg 1$. Thus, the ratio between the desired block center distance and the distance resulting from the coarse operator is

$$\frac{\Delta y\frac{1}{2}a}{2\Delta y(\frac{1}{a} + 1)} \approx \frac{a}{4}.$$

With $a \gg 1$ reflecting the aspect ratio, the crude damping factor is of order one and therefore too small to correct for the difference in block center distances and to counteract the overestimation of diffusion. The fine damping, on the other hand, corrects for the overestimation of the crude operator by using the precise geometry information.

Example 3: *Consider three quarter five-spot models with homogeneous permeability field, but physical dimension of 1, 100, and 1000 m in one direction and 1 m in the other. This gives aspect ratios of 1, 100, and 1000, respectively. Figure 6 shows the water cut curves of the simulations. The three plots indicate that increasing the aspect ratio of the reservoir, makes the difference between the crude and fine damping increasingly larger. We see that for very large aspect ratios as 1000, the crude damping fails, while the fine damping still gives reasonable results.*

Concluding remarks

In this paper we have investigated two different strategies for modeling capillary diffusion on non-uniformly coarsened grids using operator splitting between advection and diffusion. In the diffusion equation, a damping factor is needed to counteract overestimation of capillary diffusion introduced by the coarse operator. If the coarse blocks are close to a square, with approximately the same number of fine cells in each direction and aspect ratio of order one, we can use a crude damping based on the ratio of number of coarse blocks to the number of fine cells. If not, one should use a more elaborate damping that takes the local geometry of the block into account. In particular, this is necessary for reservoirs with large aspect ratios, where capillary diffusion will be greatly overestimated in one of the directions, leading to overall poor behavior of the crude damping.

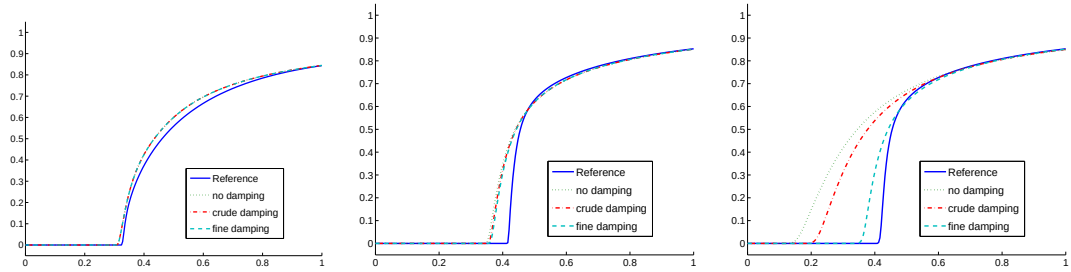

Figure 6: Water-cut curves for a homogeneous quarter five-spot with aspect ratios 1, 100, and 1000 (from left to right).

Acknowledgments: The authors would like to thank Jostein R. Natvig for valuable input to the numerical experiments. The research is funded in part by Norske Shell AS and the Research Council of Norway through grant number 175962/S30.

References

Aarnes, J.E., Hauge, V.L., and Efendiev, Y. [2007a] Coarsening of three-dimensional structured and unstructured grids for subsurface flow. *Adv. Water Resour.*, **30**(11), 2177–2193.

Aarnes, J.E., Krogstad, S., and Lie, K.A. [2007b] Multiscale mixed/mimetic methods on corner-point grids. *Computational Geosciences, Special issue on multiscale methods*, DOI: 10.1007/s10596–007–9072–8.

Christie, M.A. and Blunt, M.J. [2001] Tenth SPE comparative solution project: A comparison of upscaling techniques. *SPE Reservoir Eval. Eng.*, **4**, 308–317.

Hauge, V.L. and Aarnes, J.E. [Submitted 2007] Modeling of two-phase flow in fractured porous media on unstructured non-uniformly coarsened grids. *Transport in Porous Media*.